POPULAR SUMMARY FOR THE ARTICLE

"Improving forecast skill by assimilation of quality-controlled AIRS temperature retrievals under partially cloudy-conditions."

O. Reale, J. Susskind, R. Rosenberg, E. Brin, L.P. Riishojgaard, E. Liu, J. Terry, J.C. Jusem

The National Aeronautics and Space Administration (NASA) Atmospheric Infrared Sounder (AIRS) on board the Aqua satellite has been long recognized as an important contributor towards the improvement of weather forecasts. However, only a small fraction of the total data produced by AIRS is currently being used by operational weather systems.

In fact, in addition to effects of the procedures of thinning the data and applying quality control (which causes many data to be rejected), the only AIRS data assimilated are radiance observations of channels unaffected by clouds. This means that only the data from areas that appear cloud free at the time of the observation are being retained by operational weather forecasting systems. Therefore, being observations in mid-lower tropospheric sounding AIRS channels assimilated under completely clear-sky conditions, a very severe limitation on the horizontal distribution of the AIRS-derived information is being imposed to the atmospheric models which make use of AIRS data.

In this work it is shown that the ability to derive accurate temperature profiles from AIRS observations in partially cloud-contaminated areas can be utilized to further improve the impact of AIRS observations in a global model and forecasting system.

The analyses produced by assimilating AIRS temperature profiles obtained under partial cloud cover result in a substantially different temperature structure of the northern hemisphere lower midtroposphere at higher latitudes. This temperature difference has a strong impact, through a complex dynamical mechanism, on the representation of the polar vortex, especially over northeastern Siberia and Alaska. The polar vortex is one of the main agents of boreal winter, because on its borders most of the weather systems develop. The AIRS-induced modifications in the model representation of the polar vortex modify in turn the weather systems development and propagation through the model's dynamics, producing improved 5-day forecasts.

Improving forecast skill by assimilation of quality-controlled AIRS temperature retrievals under partially cloudy conditions.

O. Reale,[1,2] J. Susskind,[1] R. Rosenberg,[3,4] E. Brin,[3,4] L. P. Riishojgaard,[5,6,2]

E. Liu,[5,4] J. Terry,[3,4] J. C. Jusem[1,2]

O. Reale, Laboratory for Atmospheres, Code 613, NASA Goddard Space Flight Center, Greenbelt, MD 20771, USA. (Oreste.Reale-1@nasa.gov)

4   The National Aeronautics and Space Administration (NASA) Atmospheric

5   Infrared Sounder (AIRS) on board the Aqua satellite has been long recog-

6   nized as an important contributor towards the improvement of weather fore-

7   casts. At this time only a small fraction of the total data produced by AIRS

8   is being used by operational weather systems. In fact, in addition to effects

9   of thinning and quality control, the only AIRS data assimilated are radiance

[1]NASA Goddard Space Flight Center,

Laboratory for Atmospheres, Greenbelt,

Maryland, USA.

[2]University of Maryland, Baltimore

County, Baltimore, Maryland, USA.

[3]NASA Space Flight Center, Scientific

Laboratory and Visualization Office.

[4]Science Applications International

Corporation, Beltsville, Maryland, USA.

[5]NASA Space Flight Center, Global

Modeling and Assimilation Office,

Maryland, USA.

[6]Joint Center for Satellite Data

Assimilation, Camp Springs, Maryland,

USA.

10   observations of channels unaffected by clouds. Observations in mid-lower tro-

11   pospheric sounding AIRS channels are assimilated primarily under completely

12   clear-sky conditions, thus imposing a very severe limitation on the horizon-

13   tal distribution of the AIRS-derived information. In this work it is shown that

14   the ability to derive accurate temperature profiles from AIRS observations

15   in partially cloud-contaminated areas can be utilized to further improve the

16   impact of AIRS observations in a global model and forecasting system. The

17   analyses produced by assimilating AIRS temperature profiles obtained un-

18   der partial cloud cover result in a substantially colder representation of the

19   northern hemisphere lower midtroposphere at higher latitudes. This temper-

20   ature difference has a strong impact, through hydrostatic adjustment, in the

21   midtropospheric geopotential heights, which causes a different representa-

22   tion of the polar vortex especially over northeastern Siberia and Alaska. The

23   AIRS-induced anomaly propagates through the model's dynamics produc-

24   ing improved 5-day forecasts.

1. Introduction

The Aqua satellite containing the Atmospheric Infrared Sounder (AIRS) and the Advanced Microwave Sounding Unit (AMSU-A) was launched in May 2002 by the National Aeronautics and Space Administration (NASA) to become the most-advanced polar orbiting integrated infrared and microwave atmospheric sounding system to this day [Pagano et al., 2003]. The basic theory used to analyze AIRS/AMSU/HSB data in the presence of clouds, called the at-launch algorithm, and that used in a post-launch algorithm, has been described previously [Susskind et al., 2003; 2006]. The post-launch algorithm, referred to as AIRS Version 4 [Susskind et al., 2006] has been used by the NASA Goddard Distributed Active Archive Center (DAAC) to generate AIRS retrieval products. AIRS unprecedented vertical resolution allows a more detailed depiction of the thermal structure of the atmosphere with respect to other data sets such as reanalyses. For example, Tian et al. [2006] investigated the Madden Julian Oscillation and documented that AIRS-derived products improve the representation of the vertical moist thermodynamic atmospheric structure in the tropics.

Le Marshall et al. [2006] have shown an improvement of the NCEP operational system's forecasting skill resulting from the assimilation of AIRS radiance observations unaffected by clouds. Wu et al. [2006] found a specific impact on hurricane simulation by assimilating retrieved AIRS temperature and humidity profiles derived in clear conditions, which produce a more accurate representation of the Saharan Air Layer. However, despite these promising studies it should be stressed that the improved representation of the atmo-

45 spheric structure has been limited, so far, by the use of AIRS data only in areas not

46 contaminated by clouds.

47 Susskind [2007] describes some of the capabilities of the AIRS Version 5 retrieval al-

48 gorithm now being used operationally at the DAAC. A key element of the new system

49 is the ability to generate accurate case-by-case level-by-level error estimates and also use

50 them for quality control. In this work, we assimilate quality-controlled AIRS Version 5

51 temperature soundings, using the medium quality control described in Susskind [2007].

2. The Model and Data Assimilation System

52 The global data assimilation and forecasting system used is the NASA GEOS-5, which

53 combines the Gridpoint Statistical Interpolation (GSI) analysis algorithm co-developed

54 by the National Centers for Environmental Predictions (NCEP) Environmental Modeling

55 Center (documented in Wu et al., [2002]), with the NASA atmospheric global forecast

56 model, described in Bosilovich et al., [2007]. The forecast model shares the same dynami-

57 cal core [Lin, 2004] with the so-called finite-volume General Circulation Model (fvGCM),

58 used in several studies focused on tropical cyclones [e.g. Atlas et al. 2005; Shen et al.,

59 2006]. The GEOS-5 however contains a newer version of the fvGCM, differing in many

60 aspects but most notably in the physical parametrizations, partly developed by the NASA

61 Global Modeling and Assimilation Office (GMAO).

3. The Experiments

62 Three 31-day assimilation experiments, starting at 00z 1 January 2003, have been per-

63 formed with the GEOS-5 DAS run at a spatial horizontal resolution of 1°. In all three

64 experiments conventional and satellite observations used operationally at NCEP at that

65 time are assimilated, with the exclusion of AIRS data in the first run, which we define

66 CNTRL. In the second and third assimilation runs two additional sets of data are assimi-

67 lated: AIRS temperature profiles with medium quality control in one (experiment named

68 AIRS), the same AIRS data but only above 200 hPa in the other (experiment CUTF), so

69 as to assess the significance of withdrawing tropospheric temperature information derived

70 under cloudy conditions. The first four days are discarded to allow spin-up. From the

71 three sets of analyses, three corresponding sets of 27 five-day forecasts (CNTRL, AIRS

72 and CUTF) are produced and verified against operational NCEP analyses.

4. Results

73 Figure 1 shows the anomaly correlation (AC) plot for 500 hPa geopotential height in

74 the northern hemisphere extratropics, comparing 3 sets of 27 5-day forecasts: CNTRL,

75 AIRS and CUTF. The AC at day 5 (AC_5) is about .82 for the CNTRL, and a significant

76 impact of AIRS can be seen throughout the integration, with AIRS AC_5 being about .85.

77 The CUTF AC is virtually identical to that of the CNTRL, thus suggesting that most of

78 the impact during boreal winter originates from AIRS data within the troposphere.

79 The daily variation of CNTRL AC_5 between 5 and 31 January 2003 for the northern

80 hemisphere ranges between a minimum of about .67 to a maximum of .91 (Fig. 1). The

81 CUTF AC_5 does not differ remarkably from the CNTRL whereas the AIRS maintains

82 an overall superior skill, with only 5 days over 27 in which the CNTRL is better. In

83 particular, AIRS minimum and maximum AC_5s range from .76 to .91, suggesting that

84 ingestion of AIRS profiles makes the GEOS-5 system more stable.

5. Mechanism: temperature structure at the high latitudes

[85] The most relevant aspect of the AIRS data impact on the forecast is a substantially

[86] different representation of the lower midtropospheric temperature structure over the Arctic

[87] region, northeastern Asia and northern Alaska. This is observed in most of the cases in

[88] which AIRS AC_5 is higher than the CNTRL. One case is selected, initialized on January

[89] 25th, in which the difference AIRS minus CNTRL is particularly remarkable (larger than

[90] .05) and where the CNTRL performance is already satisfactory (CNTRL AC_5=.85). In

[91] other words, a case is chosen in which the ingestion of AIRS data further improves a

[92] reasonably good forecast.

[93] Fig. 2 shows the 800hPa temperature difference between AIRS and CNTRL analyses

[94] at 00z 25 January 2003: a large asymmetric temperature anomaly, slightly displaced to-

[95] wards Asia, dominates the Polar regions, with the AIRS analysis colder than the CNTRL

[96] of about 2^oC over a large portion of the Arctic and Northeastern Siberia. This remark-

[97] able temperature difference is entirely caused by AIRS data. In the same figure, the

[98] area-averaged temperature profiles for AIRS, CUTF, CNTRL and the difference AIRS

[99] minus CNTRL are computed for latitudes between 70^oN and 90^oN. The CUTF profile is

[100] virtually indistinguishable from the CNTRL up to 200hPa, confirming that most of the

[101] AIRS impact is in the troposphere. The largest difference between AIRS and CNTRL is

[102] of more than 2.5^oC between 925 hPa and 800 hPa, reaching almost 4^oC at 875hPa, and

[103] goes to zero at about 600hPa. A similar situation exists in most of the AIRS analyses

[104] associated to forecasts in which there is improvement with respect to the CNTRL (not

[105] shown).

6. Changes in the polar vortex and baroclinic waves

106   Major geopotential height hydrostatic adjustments related to the lower temperatures

107   occur in the AIRS analyses. As a consequence, the ingestion of AIRS data causes the

108   AIRS minus CNTRL 500 hPa geopotential height anomaly to be negative, on the order

109   of several tens of meters, over the entire Arctic and a fraction of northeastern Siberia

110   and Alaska (Figure 3). This difference is not found for the CUTF case which is almost

111   identical to the CNTRL (not shown).

112   The geopotential anomaly, originated mostly in the Polar regions, propagates through

113   the model forecast also in the mid-latitudes and can be followed with the aid of a Hovmøller

114   diagram (Figure 4), which shows the 500hPa geopotential AIRS minus CNTRL difference,

115   area-averaged between 40° and 80^oN. The small negative initial anomaly between 160^oE

116   and 160^oW over northeastern Siberia and Alaska corresponds well to Fig. 3, and appears

117   to undergo dispersion and propagation, producing a wave packet affecting most of North

118   America and the northern Atlantic at day 5. In the same Figure the difference between the

119   corresponding verifying NCEP analyses and the CNTRL shows a tripole between 100^oW

120   and 0° which is in qualitative good agreement with the impact induced by AIRS.

121   In Fig. 5 the 5-day 500 hPa height forecast difference between AIRS and CNTRL is

122   compared with the difference between the verifying corresponding NCEP analysis and

123   the CNTRL. A good correspondence of most features can be observed over most of the

124   western part of the northern hemisphere and over Europe, in agreement with Fig. 4. The

125   suggested explanation is that AIRS data modify the representation of the high latitude

126   low and mid-tropospheric temperature structure, leading to a substantially changed polar

127 vortex, particularly on the side of Siberia, where troughs and ridges are altered. These

128 changes in the initial conditions affect in turn baroclinic wave production and propagation

129 in the GEOS-5 forecast. Similar patterns are noted in other cases in which the AIRS AC_5

130 is larger than the CNTRL (not shown).

131 It is important to stress that the Arctic and northeastern Siberia are almost void of

132 conventional data and are not covered by geostationary data: therefore polar orbiting

133 observing systems are particularly beneficial. In our case, the data coverage provided by

134 AIRS over these regions is very dense (not shown) because of the capability of deriving

135 accurate quality controlled temperature profiles in partly cloudy conditions. Low-level

136 stratus cloud coverage over the Arctic peaks in summer but a non-negligible coverage of

137 about 18% is also documented in winter [Klein and Hartman, 1993]. The use of AIRS data

138 under partly cloudy condition allows therefore a significantly improved lower tropospheric

139 spatial coverage compared to that obtained from the use of clear-sky data only.

140 The AIRS temperature retrieval methodology involves the determination and use of

141 so-called "cloud-cleared" radiances $\hat{R}_i$ [Susskind et al., 2003], that are in effect estimates

142 of what AIRS would have measured had the scene been cloud free. These cloud-cleared

143 radiances can be assimilated in an analogous manner to that used now with cloud free

144 radiances. A comprehensive assessment of this approach will be the subject of a future

145 article.

7. Concluding Remarks

146 In this article we emphasize that the use of AIRS soundings derived in cloud contami-

147 nated areas significantly increases weather forecast skill during midlatitude boreal winter

148 conditions due to a substantially different representation of the low midtropospheric ther-

149 mal structure over the Arctic region, northeastern Siberia and Alaska. The analyzed

150 thermal anomaly induced by AIRS data ingestion causes hydrostatically related adjust-

151 ments in the representation of the mid- and upper-tropospheric height fields, modifying

152 particularly the geopotential gradients in dynamically active features such as troughs and

153 ridges. The AIRS minus CNTRL 500 hPa geopotential difference in the GEOS-5 system

154 has the appearance of a wave packet undergoing dispersion and amplification. After a

155 120 hour forecast, the modified pattern of waves and associated baroclinic weather sys-

156 tems over half of the northern hemisphere, which is caused by AIRS data ingestion, is

157 verified against the NCEP operational analyses, and found to be more realistic than the

158 control simulation without AIRS data. It is important to stress that the experiment in

159 which AIRS data are excluded only below 200 hPa is virtually indistinguishable from the

160 control and indicates that most of the AIRS impact is driven by a better depiction of the

161 troposphere, especially beneath 600 hPa.

References

164 Atlas, R., O. Reale, B.-W. Shen, S.-J. Lin, J.-D. Chern, W. Putman, T. Lee, K.-S.

165   Yeh, M. Bosilovich, and J. Radakovich, 2005: Hurricane forecasting with the high-

166   resolution NASA finite-volume general circulation model. *Geophys. Res. Letters, 32,*

167   L03807, doi:10.1029/2004GL021513.

168 Bosilovich, M. G., S.D. Schubert, M. Rienecker, R. Todling, M. Suarez, J. Bacmeister, R.

169   Gelaro, G.-K. Kim, I. Stajner, and J. Chen, 2006: NASA's Modern Era Retrospective-

170   analysis for Research and Applications. U.S. CLIVAR Variations, 4 (2), 5-8.

171 Klein, S. A., and D. L. Hartmann, (1993), The seasonal cycle of low stratiform clouds, J.

172   Climate, 6, 1587-1606.

173 Le Marshall, J., J.Jung, J.Derber, M. Chahine, R. Treadon, S. J. Lord, M. Goldberg,

174   W. Wolf, H. C. Liu, J. Joiner, J. Woollen, R. Todling, P. van Delst, and Y. Tahara

175   (2006), Improving global analysis and forecasting with AIRS *Bull. Am. Meteorol. Soc.,*

176   *87*, 747-750.

177 Lin, S.-J., 2004: A 'vertically lagrangian' finite-volume dynamical core for global models,

178   *Mon. Wea. Rev., 132*, 2293-2307.

179 Pagano, T.S., H. H. Aumann, D. E. Hagan, and K. Overoye, (2003), Prelaunch and in-

180   flight radiometric calibration of the Atmospheric Infrared Sounder (AIRS), *IEEE Trans.*

181   *Geosci. Remote Sensing, 41*, 265-273.

182 Tian, B., D. E. Waliser, E. J. Fetzer, B. H. Lambrigtsen, Y. L. Yung, and B. Wang,

183   (2006), Vertical moist thermodynamic structure and spatial-temporal evolution of the

184   MJO in AIRS observations, *J. Atmos. Sci., 63*, 2462-2485.

185 Shen, B.-W., R. Atlas, O. Reale, S.-J. Lin, J.-D. Chern, J. Chang, C. Henze, and

186   J.-L. Li, (2006), Hurricane forecasts with a global mesoscale-resolving model: Pre-

187   liminary results with Hurricane Katrina (2005), *Geophys. Res. Letters, 33*, L13813,

188   doi:10.1029/2006GL026143.

189 Susskind, J., C. Barnet, and J. M. Blaisdell, (2003), Retrieval of atmospheric and surface

190   parameters from AIRS/AMSU/HSB data in the presence of clouds. *IEEE Trans. Geosci.*

191   *Remote Sensing, 41*, 390-409.

192 Susskind, J., C. Barnet, J. Blaisdell, L. Iredell, F. Keita, L. Kouvaris, G. Molnar, and

193   M. Chahine, (2006), Accuracy of geophysical parameters derived from Atmospheric

194   Infrared Sounder/Advanced Microwave Sounding Unit as a function of fractional cloud

195   cover, *J. Geophys. Res., 111*, D09S17, doi:10.1029/2005JD006272.

196 Susskind, J., (2007), Improved atmospheric soundings and error estimates from analysis

197   of AIRS/AMSU data, Proc.of SPIE Vol. 6684, Atmospheric and Environmental Re-

198   mote Sensing Data Processing and Utilization III: Readiness for GEOSS, San Diego,

199   California, August 27-28, 2007.

200 Wu, W.-S., R.J. Purser and D.F. Parrish, (2002), Three-dimensional variational analysis

201   with spatially inhomogeneous covariances, *Mon. Wea. Rev., 130*, 2905-2916.

202 Wu, L., S. A. Braun, J. J. Qu, and X. Hao, (2006), Simulating the formation

203   of Hurricane Isabel (2003) with AIRS data. *Geophys. Res. Lett., 33*, L04804,

204   doi:10.1029/2005GL024665.

grl_fig01.eps
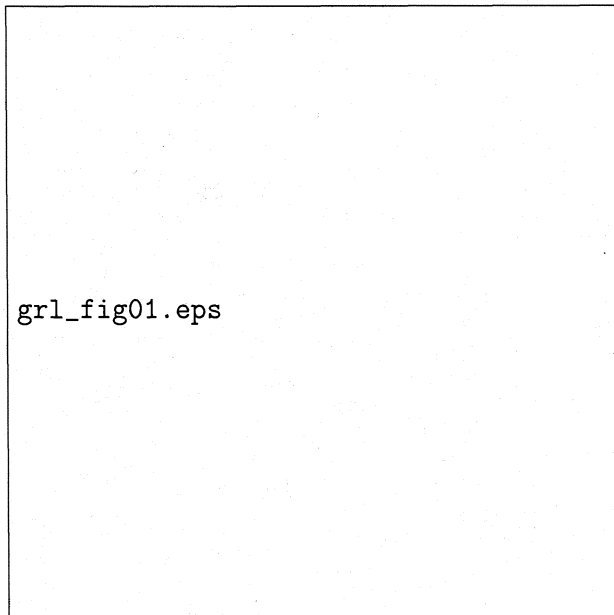
Figure 1.   500 hPa geopotential height anomaly correlation for the Northern Hemisphere Extratropics (above), north of $30^{o}N$. Green is AIRS, red is CUTF, black is CNTRL. Time series of 500NHAC (below). The numbers refer to individual forecasts. Case n.1 corresponds to January 5th. The thick line on n.21 corresponds to the selected case of January 25th.

grl_fig02.eps
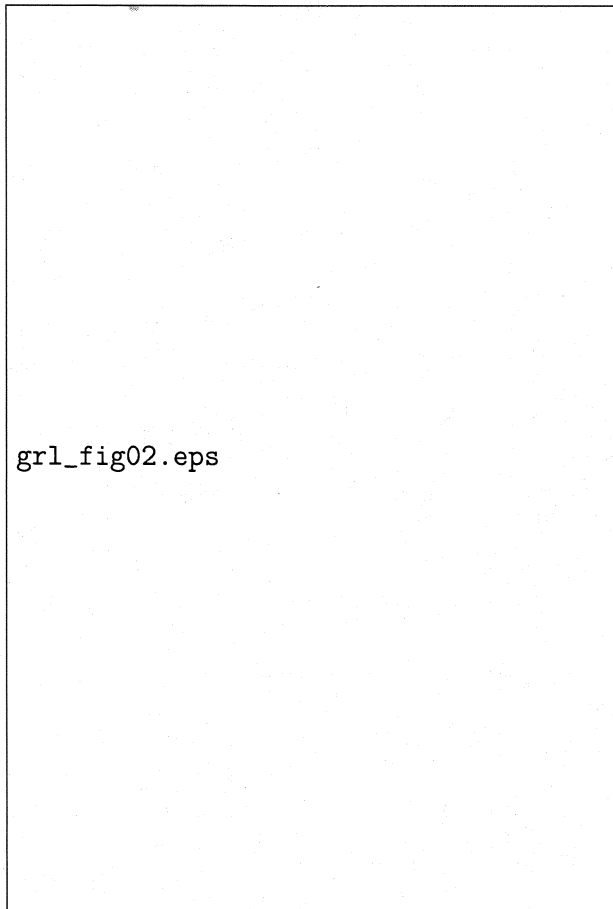
Figure 2. Temperature anomaly analyses (AIRS minus CNTRL, ^oC, above) at 800hPa and area-averaged ($70^o - 90^oN$) temperature (^oC) vertical profiles from analyses at 00z 25 January (below). CUTF and CNTRL virtually indistinguishable below 200hPa. Upper horizontal axis refers to CNTRL, AIRS, CUTF, lower horizontal axis in red refers to AIRS minus CNTRL.
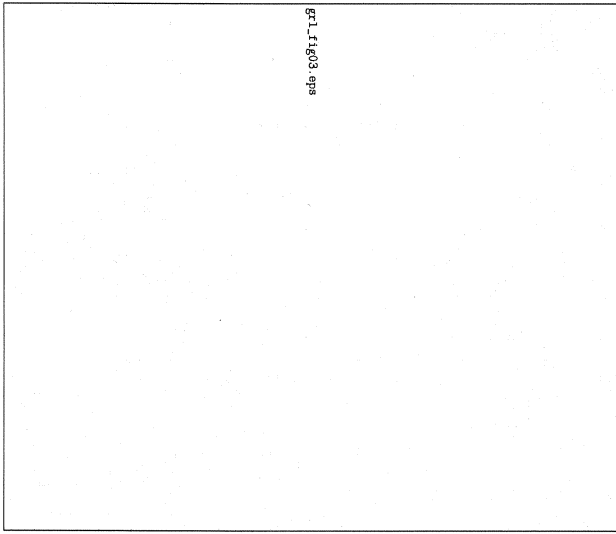
Figure 3. Geopotential height (*m*) anomaly analysis (AIRS minus CNTRL) at 500 hPa, 00z 25 January.
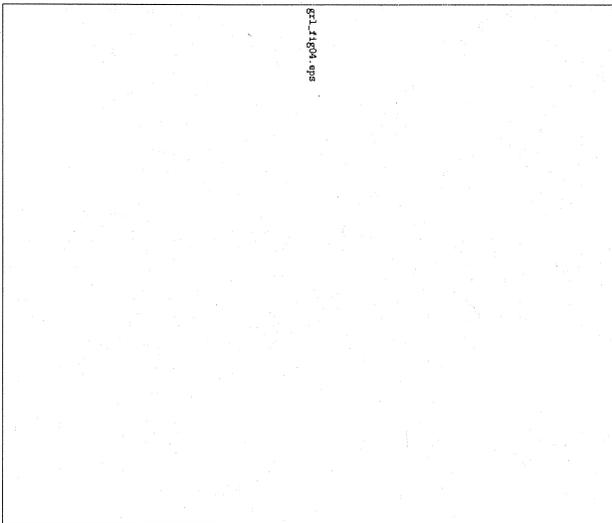
Figure 4. Hovmøller diagram of latitudinally-averaged ($40^o - 80^o$) 500hPa height (*m*) anomaly forecast (AIRS-CNTRL) from 00z 25 January to 06z 30 January (shaded). Difference between NCEP verifying analyses and CNTRL forecast is superimposed (solid contour). Time upward.

grl_fig05.eps
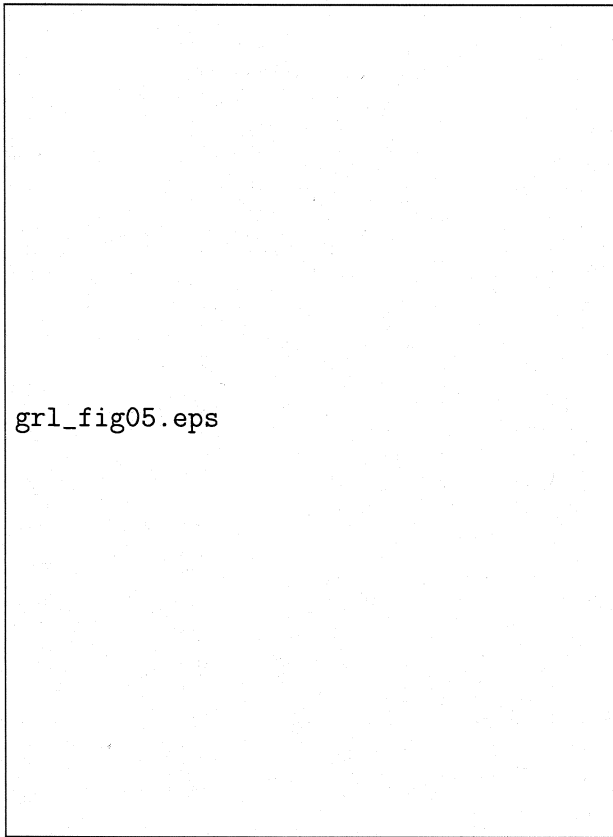
Figure 5.   500hPa height (*m*) anomaly 120h forecast (AIRS minus CNTRL, shaded, panel

above) and NCEP verifying analyses minus CNTRL 120h forecast (shaded, below) at verifying

time of 00z 30 January. On both panels the corresponding CNTRL 500hPa geopotential 120h

forecast (initialized at 00z 25 Jan, contour) is superimposed. Latitude range $25^o - 70^oN$ for

clarity.
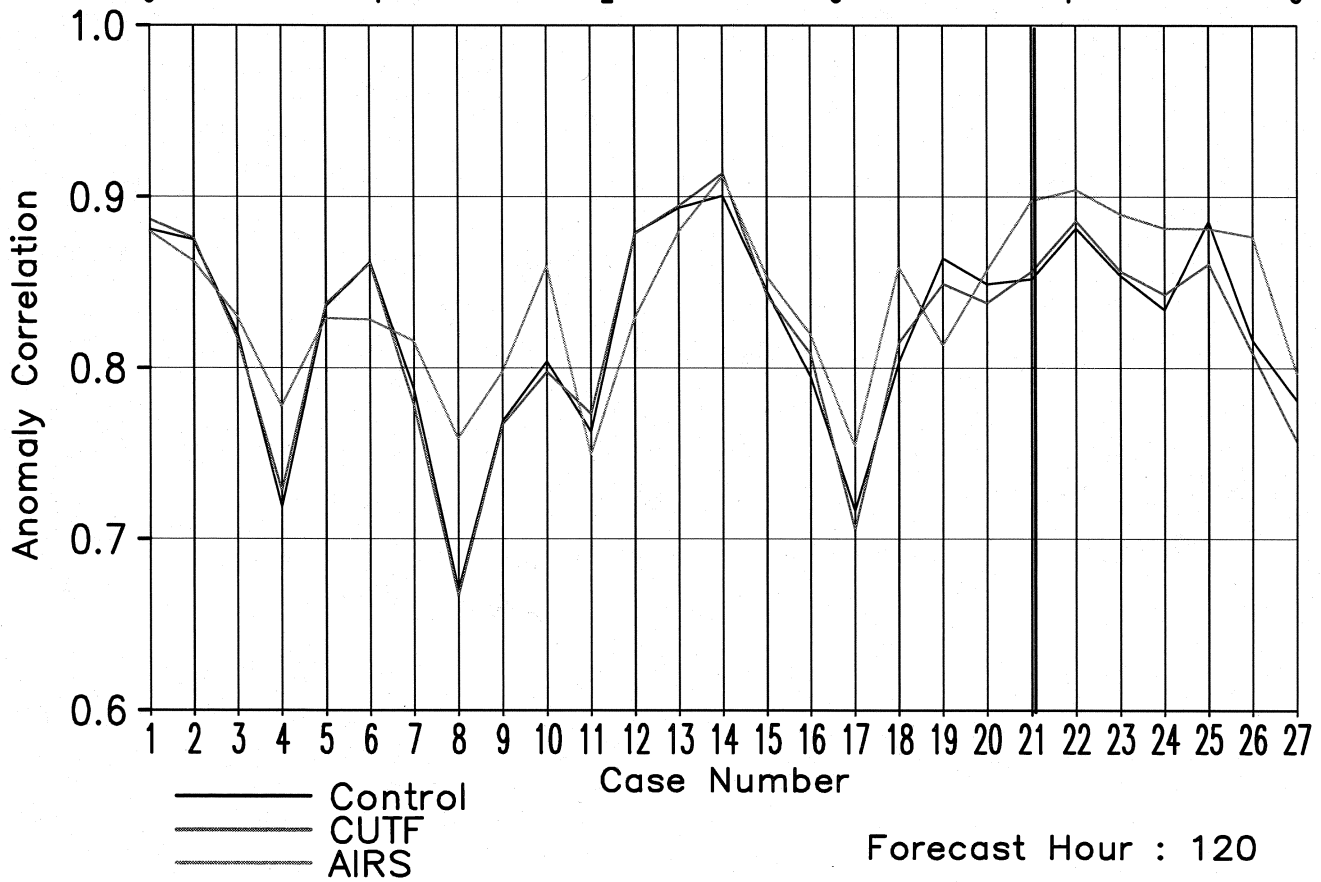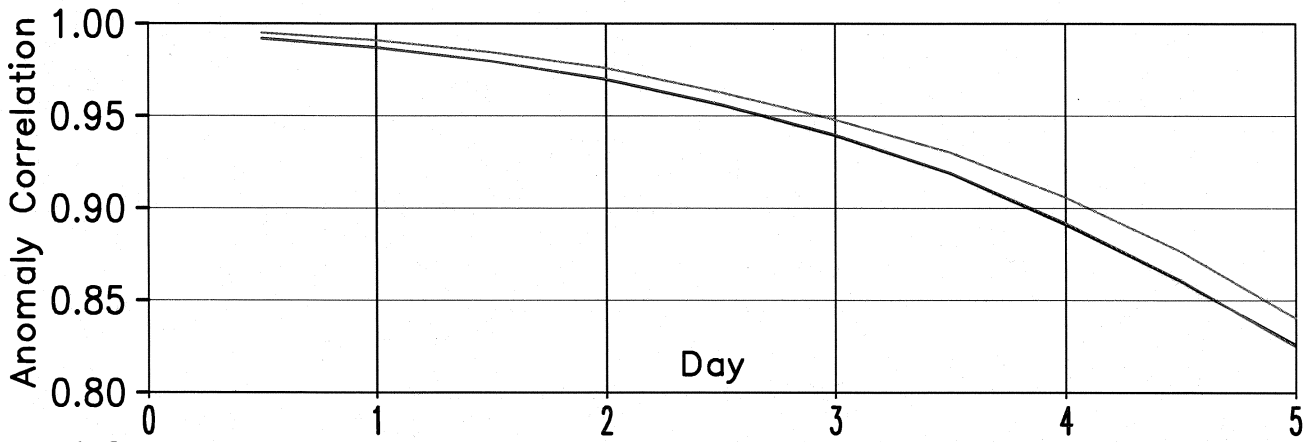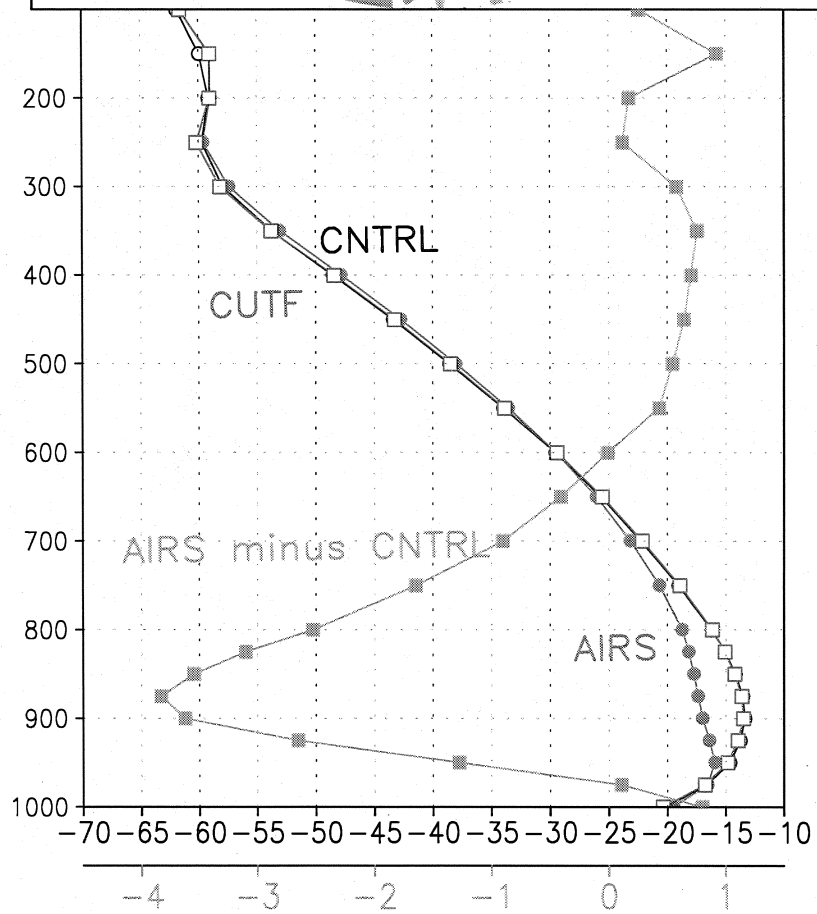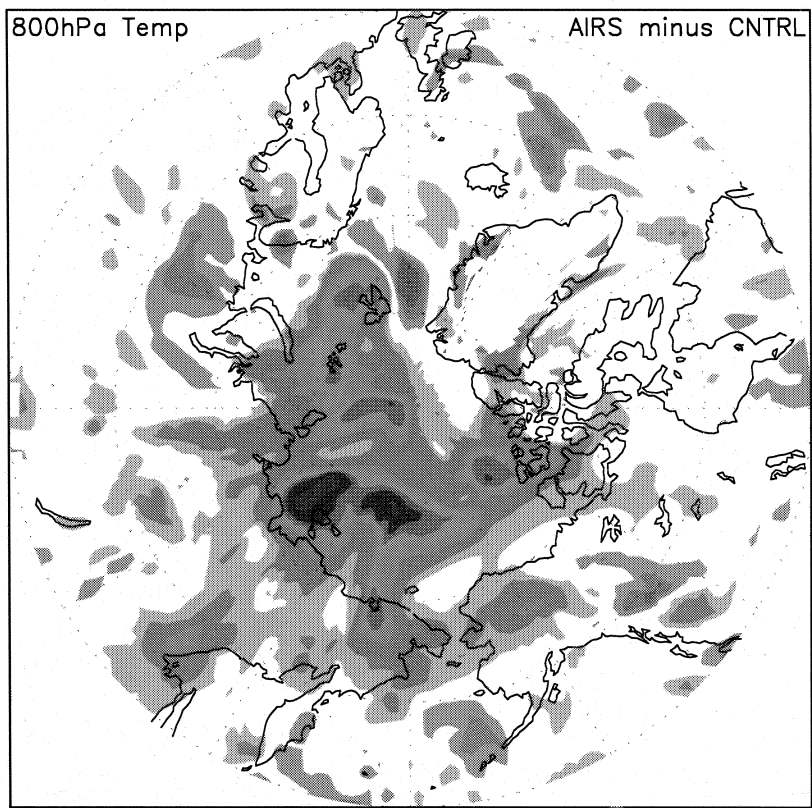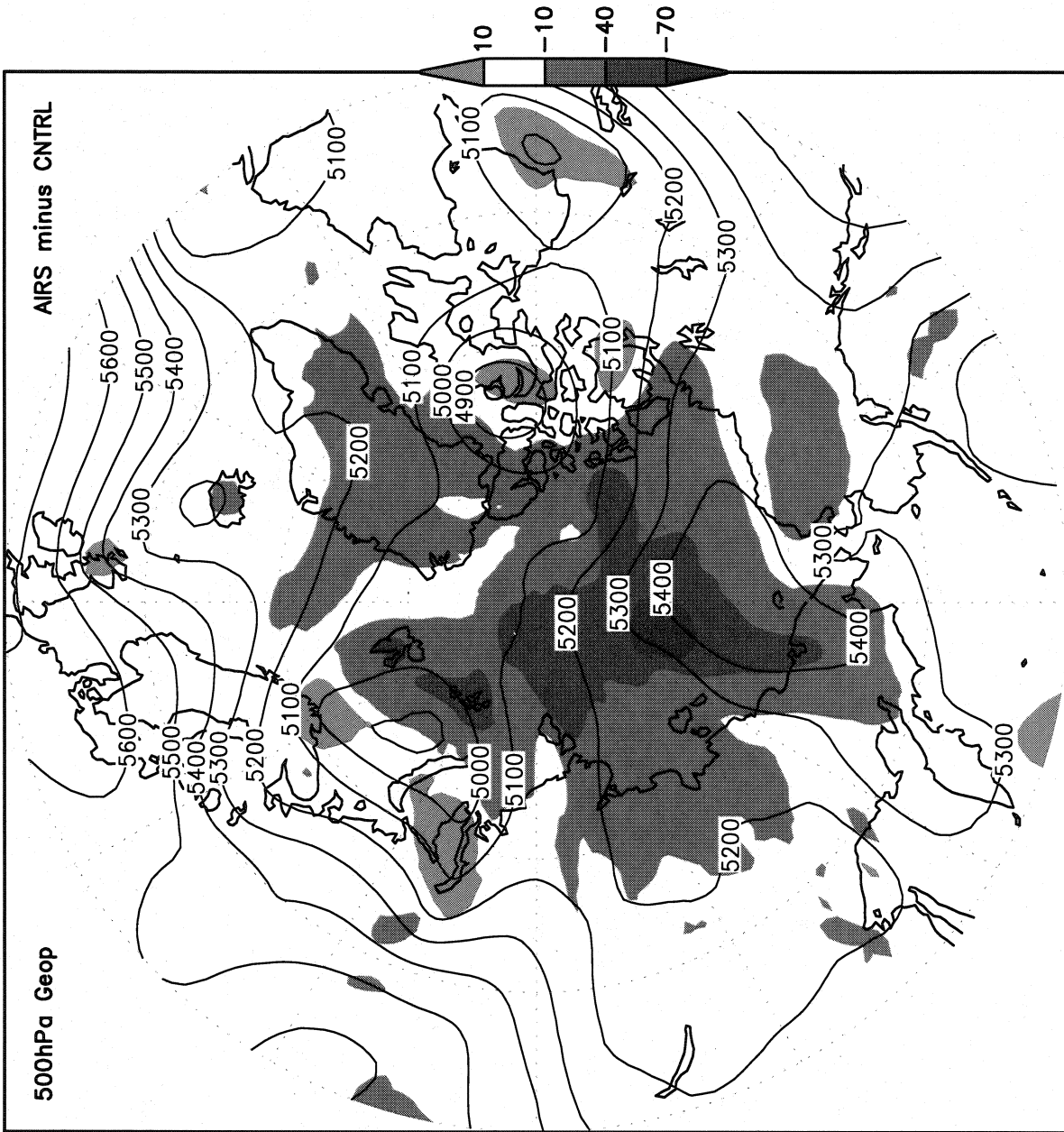
500hPa AIRS minus Control Latavgd 40-80N

500hPa Geop   5600   5400   AIRS minus CNTRL

500hPa Geop   5600   5400   NCEP minus CNTRL